Cooperation of the NEIL3 and Fanconi Anemia/BRCA Pathways in Interstrand Crosslink Repair

Niu Li[1,2,3], Jian Wang[1], Susan S. Wallace[4], Jing Chen[2], Jia Zhou[3,*], Alan D. D'Andrea[3,5,6,*]

1 Department of Medical Genetics and Molecular Diagnostic Laboratory, Shanghai Children's Medical Center, Shanghai Jiaotong University School of Medicine, Shanghai, China
2 Key Laboratory of Pediatric Hematology and Oncology Ministry of Health, Department of Hematology and Oncology, Shanghai Children's Medical Center, Shanghai Jiao Tong University School of Medicine, Shanghai, China
3 Department of Radiation Oncology, Dana-Farber Cancer Institute, Harvard Medical School, Boston, MA, USA
4 Department of Microbiology and Molecular Genetics, University of Vermont, Burlington, VT, USA
5 Center for DNA Damage and Repair, Dana-Farber Cancer Institute, Harvard Medical School, Boston, MA, USA
6 Susan F. Smith Center for Women's Cancers, Dana-Farber Cancer Institute, Harvard Medical School, Boston, MA, USA
* co-corresponding authors

Corresponding Authors:
Alan D. D'Andrea, M.D.
Director: Center for DNA Damage and Repair
The Fuller-American Cancer Society Professor
Harvard Medical School
Chief, Division of Genomic Stability and DNA Repair
Department of Radiation Oncology
Dana-Farber Cancer Institute, HIM243
450 Brookline Ave.
Boston, MA 02215
617-632-2080
FAX: 617-632-6069
Alan_Dandrea@dfci.harvard.edu

Jia Zhou, Ph.D.
Department of Radiation Oncology
Dana-Farber Cancer Institute
Harvard Medical School
617-582-8523
jia_zhou@dfci.harvard.edu

Running Title: NEIL3 pathway is prioritized in psoralen-ICL Repair

Key Words: NEIL3, Fanconi Anemia, Psoralen Interstrand crosslink

Supplementary Figure Legends

Figure S1: Sensitivity of NEIL3 depleted cells to DNA damaging agents. **(A)** The viability of WT and *NEIL3*$^{-/-}$ HeLa cells after the treatment of various DNA damaging agents, including PUVA, MMC, cisplatin, HU, camptothecin, IR, UVB, psoralen, and UVA. **(B)** Cell viability was monitored in HeLa or U2OS cells after treatment of psoralen or UVA. **(C)** Cell viability was measured in the SV40-immortalized WT and *Neil3*$^{-/-}$-MEF cells after treatment with PUVA, psoralen or UVA. **(D)** Cell viability was monitored in HeLa-WT, HeLa- FANCA$^{-/-}$, and HeLa-*NEIL3*$^{-/-}$ cells after MMC or cisplatin treatment. **(E)** Cell viability was monitored after NEIL3 knockdown and PUVA treatment in PD20 plus empty vector (PD20-EV) and PD20 plus FANCD2 (PD20-D2) cells. Shown on the right, immunoblotting was used to evaluate the knockdown efficiency of NEIL3 and to evaluate FANCD2 complementation. **(F)** MMC and cisplatin sensitivities were monitored after knockdown of FANCD2 in HeLa-WT and HeLa-*NEIL3*$^{-/-}$ cells, respectively. Data are mean ± s.e.m. from three independent experiments. **(G)** Sensitivity of HeLa cells to PUVA after NEIL1 or control knockdown. HeLa cells were transfected with control or NEIL1 siRNA (20 nM siRNA, see Table S1 for sequence). Cells were treated with PUVA using indicated doses, and cell viability was measured 4 days after treatment. NEIL1 knockdown efficiency was evaluated at mRNA level, and NEIL3 mRNA level was determined after knockdown of NEIL1 in HeLa cells by quantitative RT-PCR. Primer sequences can be found in the Materials and Methods.

Figure S2: Response of NEIL3 to psoralen-ICLs was independent of cell cycle. **(A)** The NEIL3 expression level was determined in WT and FANCA$^{-/-}$ HeLa cells after treatment with indicated dose of psoralen or UVA (0.8 J/cm^2). **(B)** The protein expression level of NEIL3 was increased after FANCD2 complementation in PD20 cells and FANCG complementation in PD326 cells. **(C)** The *NEIL3* mRNA level was determined in wild-type and FA/BRCA-deficient (FANCD2$^{-/-}$ or FANCA$^{-/-}$) cells. **(D)** HeLa cells were synchronized by double-thymidine blocks (2 mM) and released into fresh medium, and cell cycle were analyzed at 0, 2, 4, 8 h after releasing. NEIL3 protein levels were determined at different cell cycle stages. **(E, F)** Cell cycle was analyzed in HeLa/HeLa-FANCA$^{-/-}$ and U2OS/U2OS-FANCD2$^{-/-}$ cells.

(G) WT or *FANCD2*$^{-/-}$ U2OS (left) and WT or *NEIL3*$^{-/-}$ HeLa cells (right) were treated with 20 μM MG-132 and collected at indicated time. Cell lysates were analyzed by Western blot using indicated antibody. **(H)** Left, co-IP was performed using normal IgG, anti-NEIL3, anti-FANCD2, or anti-FANCG antibodies in 293T cells lysates. The input and co-IP samples were analyzed by Western blot using indicated antibodies. The FANCA-FANCD2 and FANCA-FANCG interactions served as positive controls. Right, 293T cells were transiently transfected with indicated plasmids, and one group was treated with 100 ng/ml MMC for 6 h. The input and co-IP samples were analyzed by Western blot using anti-FANCD2 and anti-HA antibodies. **(I, J)** Cell cycle was analyzed in HeLa and HeLa-FANCA$^{-/-}$ cells after treatment with PUVA (50 nM psoralen plus 0.8 J/cm^2 UVA) for 24 h.

Figure S3: γH2AX foci analysis in FANCA$^{-/-}$ and NEIL3$^{-/-}$ cells upon PUVA and MMC treatments.

(A) Representative images of immunofluorescence assays (IFA) showing γH2AX foci at 0 and 24 hours after PUVA in the HeLa-WT, HeLa-*FANCA*$^{-/-}$ and HeLa-*NEIL3*$^{-/-}$ cells. **(B)** γH2AX foci formation in HeLa and HeLa-*NEIL3*$^{-/-}$ cells after siFANCD2 and PUVA. 48 h after siControl or siFANCD2 transfection, cells were treated with PUVA and allowed to recover for 20 h before fixation and γH2AX detection. γH2AX foci was detected by IFA. **(C)** IFA images showing γH2AX foci at 24 h in the HeLa, HeLa-FANCA$^{-/-}$ and HeLa-NEIL3$^{-/-}$ cells after being treated with 5 ng/mL MMC. **(D)** Quantification of the γH2AX foci at 0, 6, and 20 h after treatment with 5 ng/mL MMC in HeLa-WT, HeLa-FANCA$^{-/-}$ and HeLa-NEIL3$^{-/-}$ cells. Data shown are mean ± s.e.m. from three independent experiments.

Figure S4: The recruitment of NEIL3 and FANCD2 were mutually independent. **(A)** The Expression of EGFP-NEIL3 plasmids in U2OS cells was validated by Western blot. **(B)** UVA alone does not trigger the recruitment of NEIL3. NEIL3-EGFP was transfected into U2OS cells, and UVA laser striping was performed in the presence and absence of psoralen. Representative images and quantification of cells (n = 50) with positive NEIL3-EGFP recruitment were shown. **(C)** Effects of ATM, ATR, and DNPK inhibitors on NEIL3 recruitment to psoralen-ICLs. U2OS cells expressing NEIL3-EGFP were pre-incubated with 10 μM psoralen and the

recruitment of NEIL3 was visualized 1 min after exposure to UVA laser. ATM inhibitor (KU-55933), ATR inhibitor (Berzosertib), or DNPK inhibitor (Nedisertib), was added 1 hour before laser striping. Representative images of NEIL3-EGFP recruitment and quantification of cells with positive NEIL3 recruitment to psoralene-ICL laser tracts were shown. A total of 100 cells were quantified for each group. **(D)** The Expression of EGFP-NEIL3 plasmids in U2OS cells was validated by Western blot. **(E)** The protein levels of PARP1 and PARP3 were determined after knockdown of PARP1 or PARP3 in the U2OS cells. **(F, G)** Laser striping was used to analyze the recruitment efficiency of NEIL3 (F) and FANCD2 (G) after knockdown of PARP1 or PARP3. A total of 100 cells were counted for each group. n.s., no significance, **, $p < 0.01$; ***, $p < 0.001$ (paired t test). **(H)** Laser striping analysis of the recruitment of EGFP-FANCD2 in U2OS-NEIL3$^{-/-}$ cells. **(I)** Laser striping experiments were performed to determine the recruitment of NEIL3-EGFP in U2OS-FANCD2$^{-/-}$ cells.

Figure S5: Contribution of the RUVBL1/RUVBL2 complex in ICLs repair via the NEIL3 pathway and the FA pathway. **(A)** The NEIL3-GFP pulldown samples were separated by SDS-PAGE gel electrophoresis and were examined by silver staining. Red arrow, the bait NEIL3-GFP. UT, untreated, PUVA, psoralen plus UVA. **(B)** List of the top candidate interactors of NEIL3 from mass spectrum analysis**. (C)** Immunoblot validation of the expression of the RUVBL1-Flag and RUVBL2-Flag constructs. RUVBL1, RUVBL2 and Flag antibodies were used. **(D, E)** Laser striping to analyze the recruitment of NEIL3 (D) and FANCD2 (E) in U2OS cells after knockdown of RUVBL1 or RUVBL2 using siRNA. A total of 100 cells were counted for each group. n.s., no significance (paired t-test). **(F)** Mono-ubiquitination of FANCD2 and FANCI was analyzed in HeLa and U2OS cells after knockdown of RUVBL1 or RUVBL2 and treatment with 50 ng/ml MMC for 24 h. **(G)** RUVBL1 and RUVBL2 protein levels were analyzed in WT, *FANCA*$^{-/-}$, and *FANCD2*$^{-/-}$ cells. **(H)** Cell cycle analysis of HeLa cells that were treated with siControl or siRUVBL1. **(I, J)** Cell viability was measured after knockdown of RUVBL1 (or RUVBL2) and treatment with MMC, in HeLa-*NEIL3*$^{-/-}$ (H) and HeLa-*FANCA*$^{-/-}$ (I) cells and their WT counterparts.

Figure S6: NEIL3 recruitment after depletion of TRAIP and MCM7. **(A)** Quantitative RT-

PCR (qRT-PCR) was used to determine the knockdown efficiency of the TRAIP siRNA in HeLa cells, due to the lack of a good antibody. **(B)** HeLa cells were co-transfected with a TRAIP-Myc plasmid and siControl or siTRAIP siRNAs. The exogenous expression of TRAIP-Myc and knockdown of TRAIP were confirmed by immunoblotting the Myc-tag. **(C)** MCM7 siRNA knockdown was analyzed by immunoblot in cell lysates from HeLa. Laser striping was performed to analyze the recruitment efficiency of EGFP-NEIL3 in U2OS cells after MCM7 knockdown. A total of 100 cells were counted for each group. *, $p < 0.05$ (paired t test). (**D**-**E**) Microscopic images of NEIL3-GFP (D) and FANCD2-GFP (E) recruitment to laser stripes before and after PUVA laser. Cells were treated with indicated siRNA before PUVA laser striping.

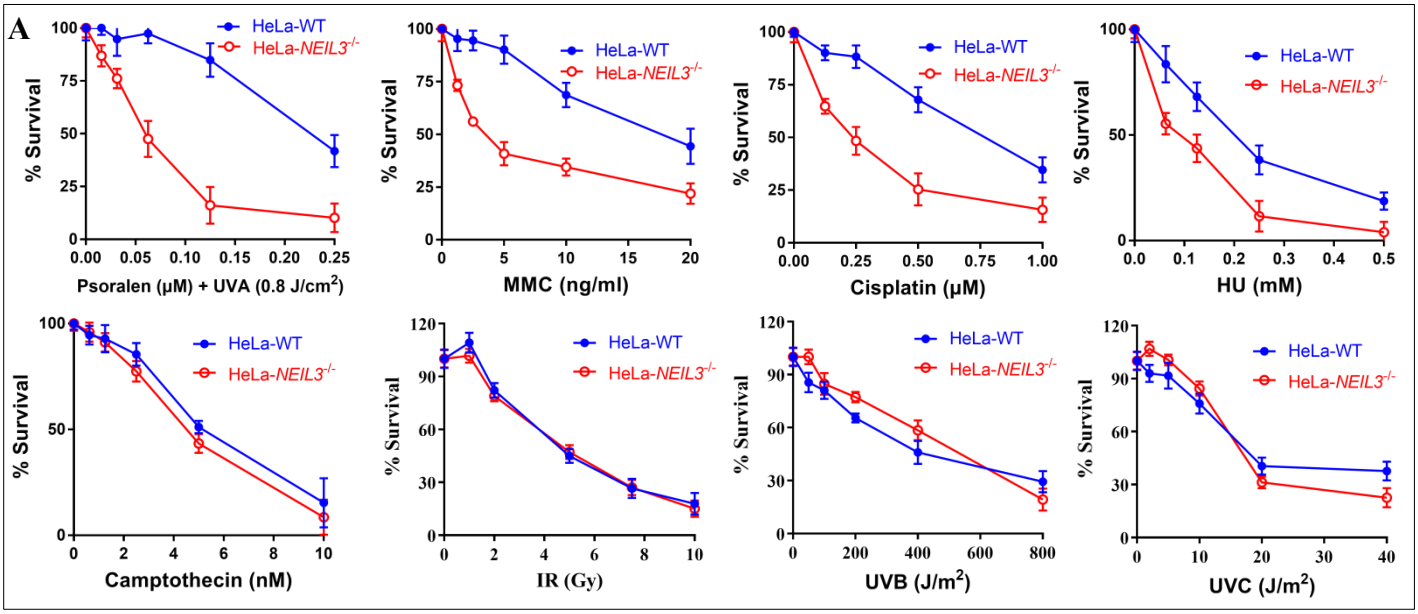
A
HeLa-WT
HeLa-NEIL3-/-
% Survival
Psoralen (μM) + UVA (0.8 J/cm2)
MMC (ng/ml)
Cisplatin (μM)
HU (mM)
Camptothecin (nM)
IR (Gy)
UVB (J/m2)
UVC (J/m2)

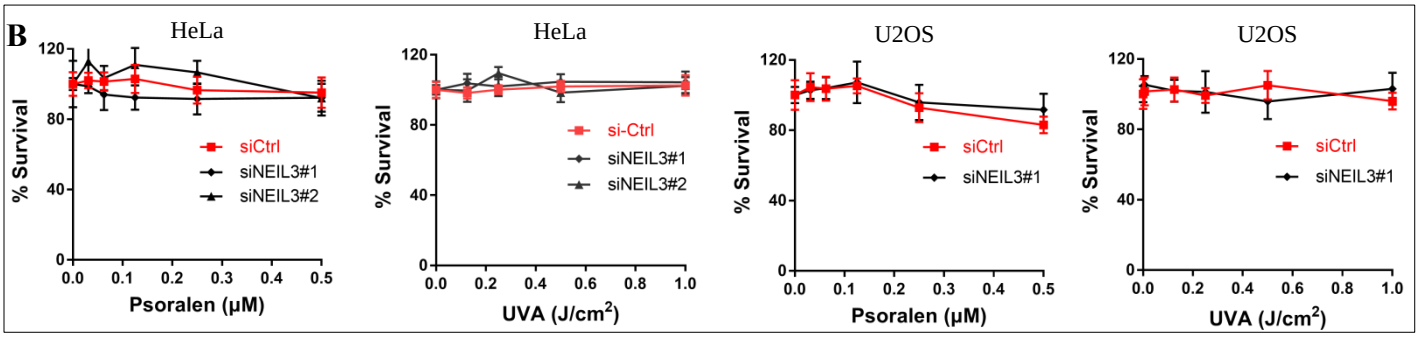
B
HeLa
U2OS
siCtrl
siNEIL3#1
siNEIL3#2
si-Ctrl
% Survival
Psoralen (μM)
UVA (J/cm2)

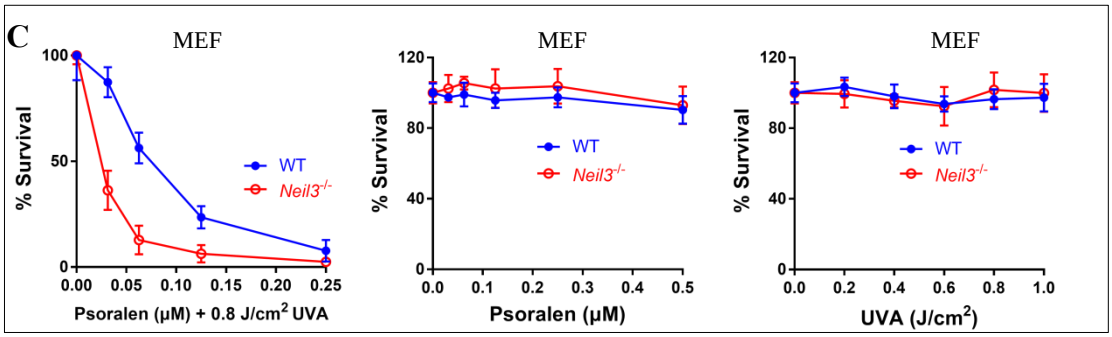
C
MEF
WT
Neil3-/-
% Survival
Psoralen (μM) + 0.8 J/cm2 UVA
Psoralen (μM)
UVA (J/cm2)

Figure S1

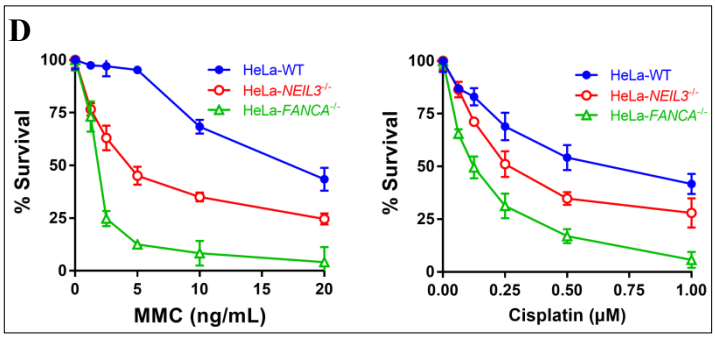
D
HeLa-WT
HeLa-NEIL3-/-
HeLa-FANCA-/-
% Survival
MMC (ng/mL)
Cisplatin (μM)

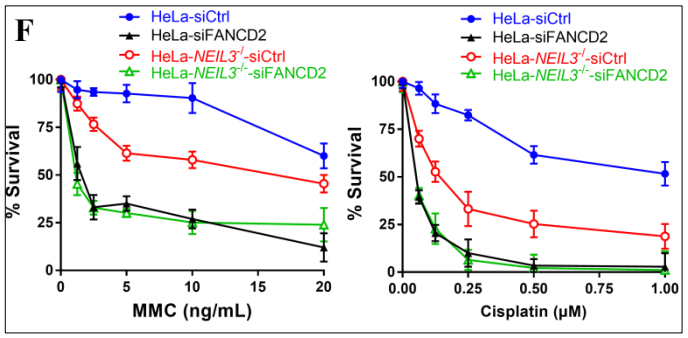
F
HeLa-siCtrl
HeLa-siFANCD2
HeLa-NEIL3-/--siCtrl
HeLa-NEIL3-/--siFANCD2
% Survival
MMC (ng/mL)
Cisplatin (μM)

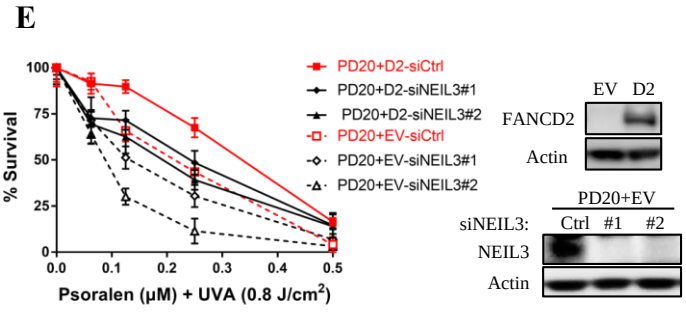
E
PD20+D2-siCtrl
PD20+D2-siNEIL3#1
PD20+D2-siNEIL3#2
PD20+EV-siCtrl
PD20+EV-siNEIL3#1
PD20+EV-siNEIL3#2
% Survival
Psoralen (μM) + UVA (0.8 J/cm2)
EV
D2
FANCD2
Actin
PD20+EV
siNEIL3:
Ctrl
#1
#2
NEIL3
Actin

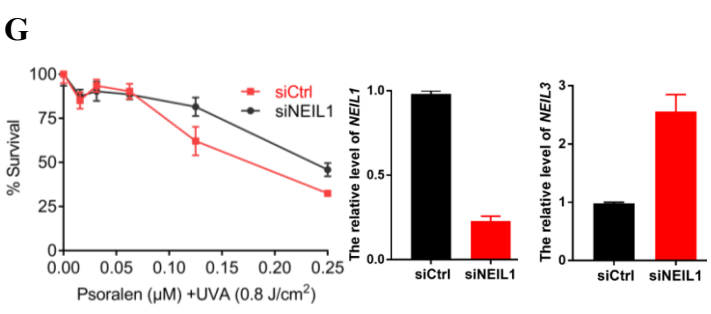
G
siCtrl
siNEIL1
% Survival
Psoralen (μM) +UVA (0.8 J/cm2)
The relative level of NEIL1
The relative level of NEIL3

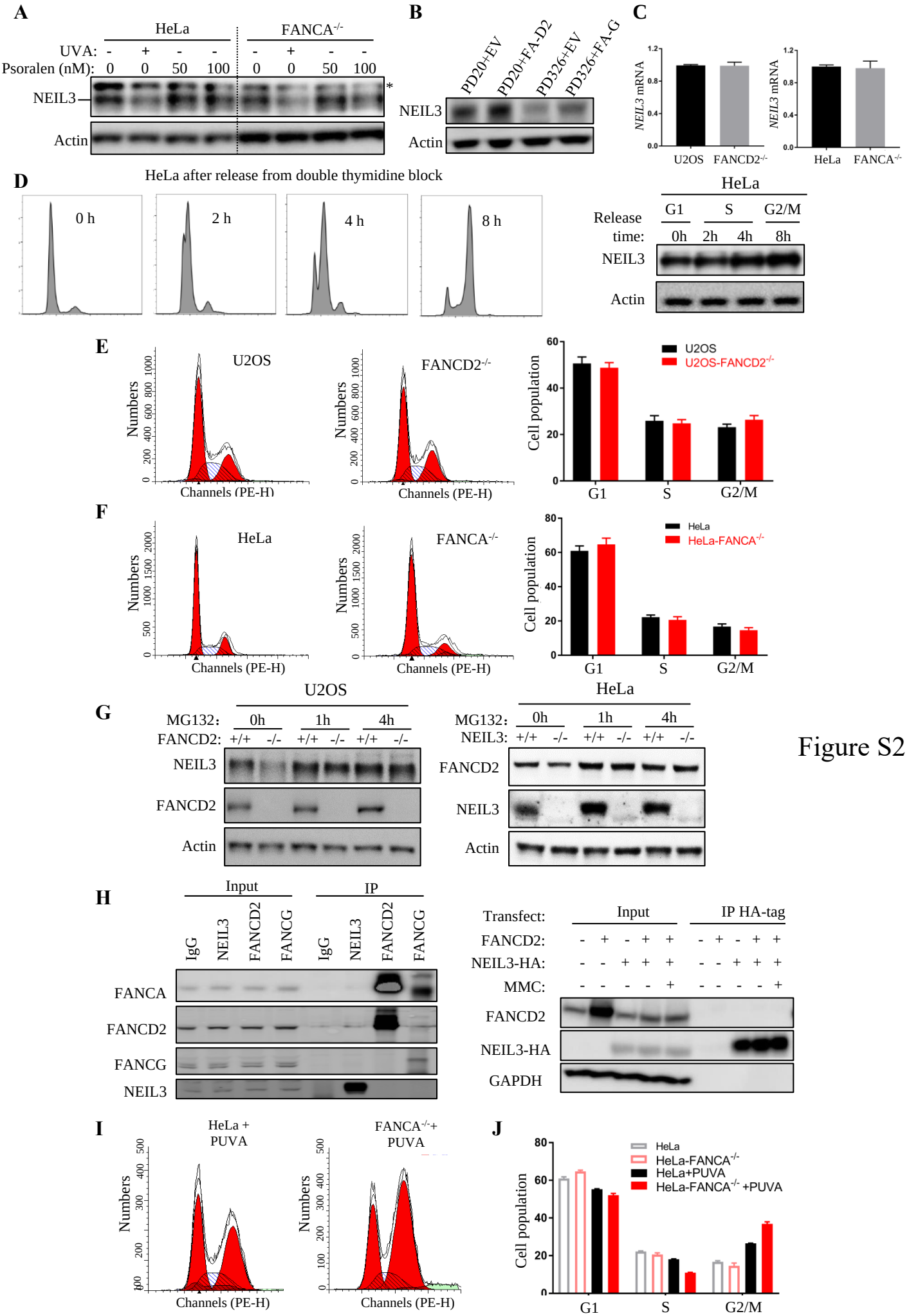
A
HeLa
FANCA-/-
UVA: - + - - - + - -
Psoralen (nM): 0 0 50 100 0 0 50 100
NEIL3
Actin
B
PD20+EV
PD20+FA-D2
PD326+EV
PD326+FA-G
NEIL3
Actin
C
NEIL3 mRNA
U2OS
FANCD2-/-
HeLa
FANCA-/-
D
HeLa after release from double thymidine block
0 h
2 h
4 h
8 h
HeLa
Release time:
G1
S
G2/M
0h 2h 4h 8h
NEIL3
Actin
E
U2OS
FANCD2-/-
Numbers
Channels (PE-H)
Cell population
U2OS
U2OS-FANCD2-/-
G1
S
G2/M
F
HeLa
FANCA-/-
HeLa-FANCA-/-
G
U2OS
HeLa
MG132:
FANCD2:
NEIL3:
0h 1h 4h
NEIL3
FANCD2
Actin
H
Input
IP
IgG
NEIL3
FANCD2
FANCG
FANCA
Transfect:
FANCD2:
NEIL3-HA:
MMC:
IP HA-tag
GAPDH
I
HeLa + PUVA
FANCA-/-+ PUVA
J
HeLa
HeLa-FANCA-/-
HeLa+PUVA
HeLa-FANCA-/- +PUVA

Figure S2

Figure S3

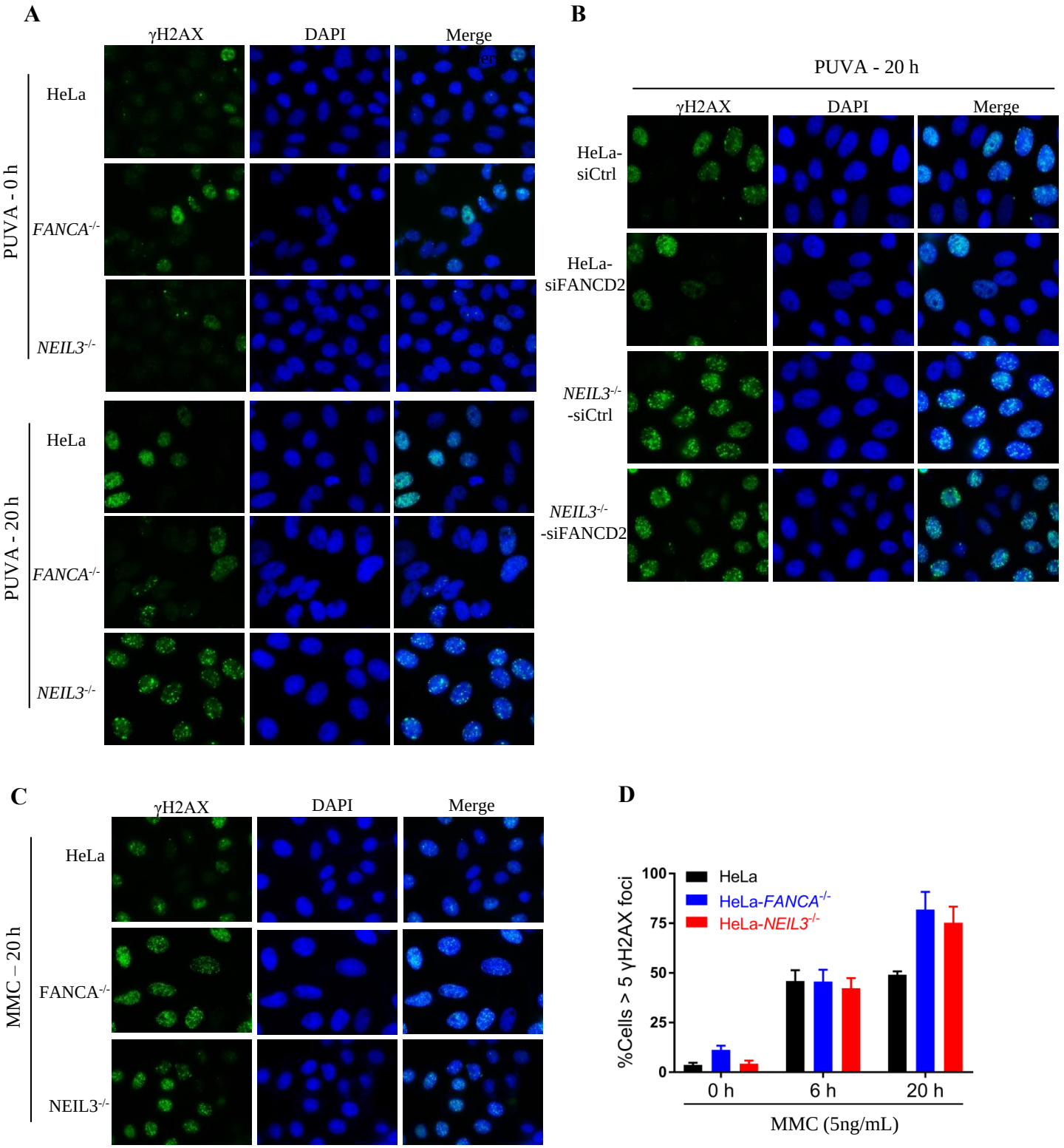
A
γH2AX
DAPI
Merge
PUVA - 0 h
HeLa
FANCA-/-
NEIL3-/-
PUVA - 20 h
HeLa
FANCA-/-
NEIL3-/-
B
PUVA - 20 h
γH2AX
DAPI
Merge
HeLa-siCtrl
HeLa-siFANCD2
NEIL3-/- -siCtrl
NEIL3-/- -siFANCD2
C
γH2AX
DAPI
Merge
MMC – 20 h
HeLa
FANCA-/-
NEIL3-/-
D
%Cells > 5 γH2AX foci
100
75
50
25
0
HeLa
HeLa-FANCA-/-
HeLa-NEIL3-/-
0 h
6 h
20 h
MMC (5ng/mL)

Figure S4

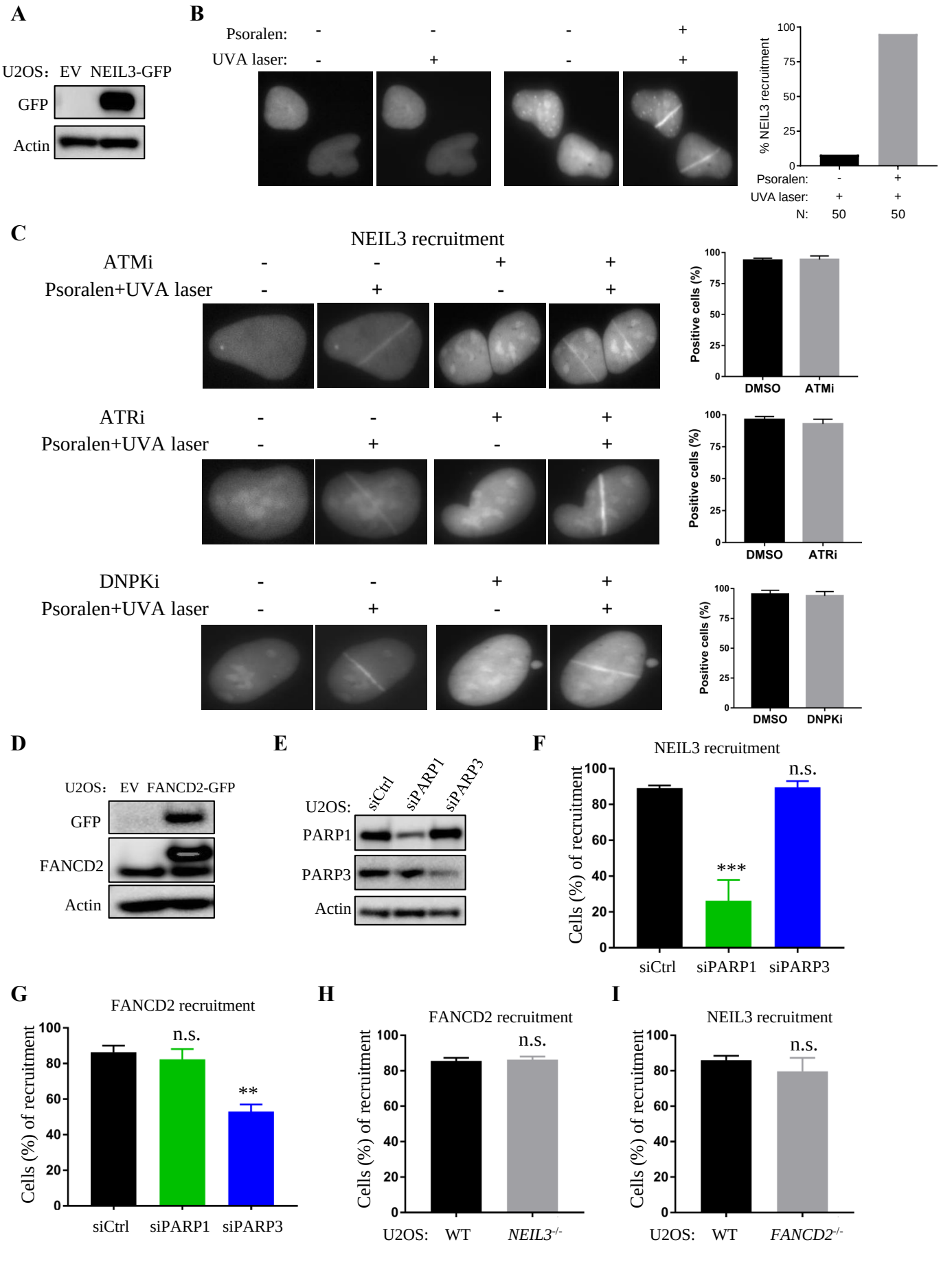
A
U2OS: EV NEIL3-GFP
GFP
Actin
B
Psoralen: - - - +
UVA laser: - + - +
% NEIL3 recruitment
100
75
50
25
0
Psoralen: - +
UVA laser: + +
N: 50 50
C
NEIL3 recruitment
ATMi - - + +
Psoralen+UVA laser - + - +
Positive cells (%)
DMSO ATMi
ATRi - - + +
Psoralen+UVA laser - + - +
DMSO ATRi
DNPKi - - + +
Psoralen+UVA laser - + - +
DMSO DNPKi
D
U2OS: EV FANCD2-GFP
GFP
FANCD2
Actin
E
U2OS: siCtrl siPARP1 siPARP3
PARP1
PARP3
Actin
F
NEIL3 recruitment
Cells (%) of recruitment
n.s.
***
siCtrl siPARP1 siPARP3
G
FANCD2 recruitment
Cells (%) of recruitment
n.s.
**
siCtrl siPARP1 siPARP3
H
FANCD2 recruitment
Cells (%) of recruitment
n.s.
U2OS: WT NEIL3-/-
I
NEIL3 recruitment
Cells (%) of recruitment
n.s.
U2OS: WT FANCD2-/-

Figure S5

A

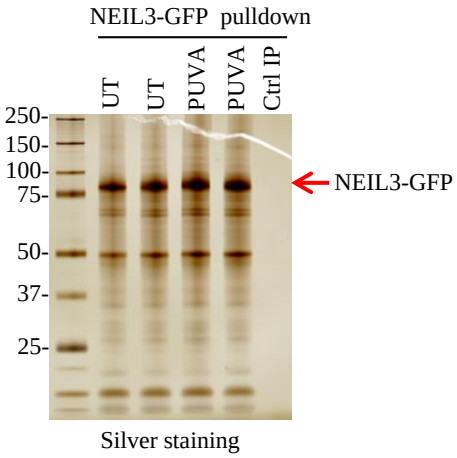

B

	Unique Peptide		
Top 10 genes	Control IP	Untreated	PUVA
NEIL3	6	40	44
RUVBL2	3	39	50
SNRPA1	1	10	12
XRCC5	1	19	37
XRCC6	2	18	32
UBA52	2	7	5
HSP90AA1	6	17	25
DHX9	3	25	33
HSP90AB1	5	7	10
HNRNPF	2	18	27
Other genes			
RUVBL1	0	31	32
PARP1	6	26	28

C

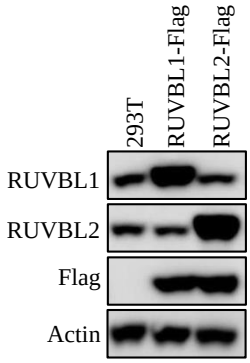

D

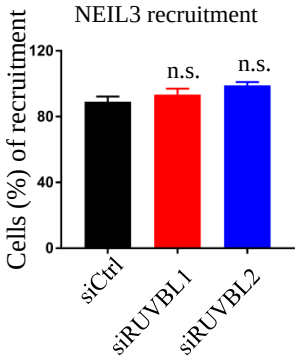

E

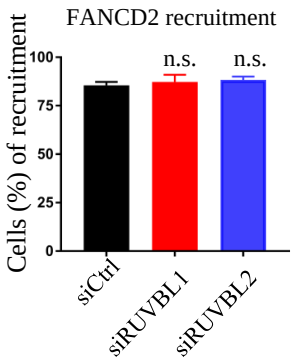

F

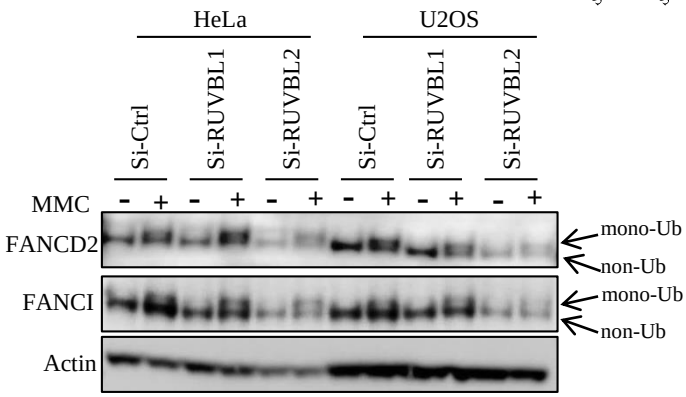

G

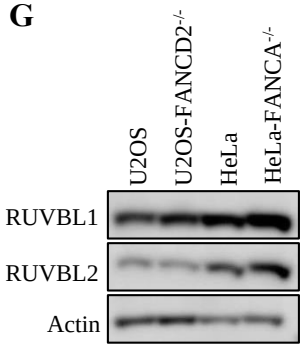

H

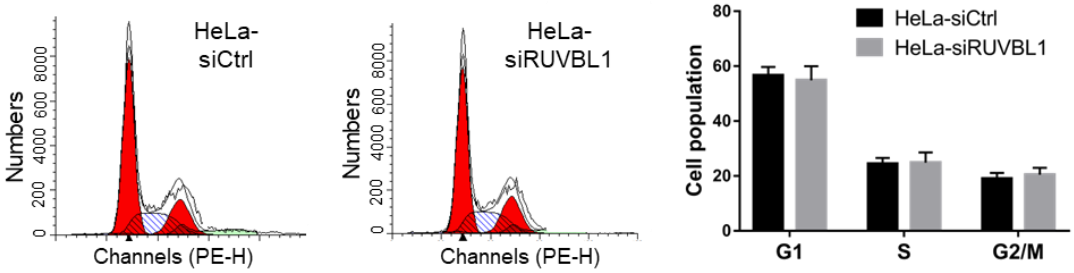

I

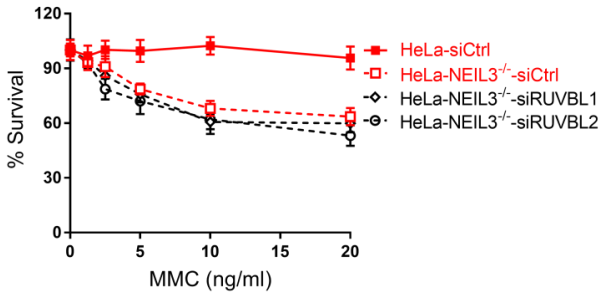

J

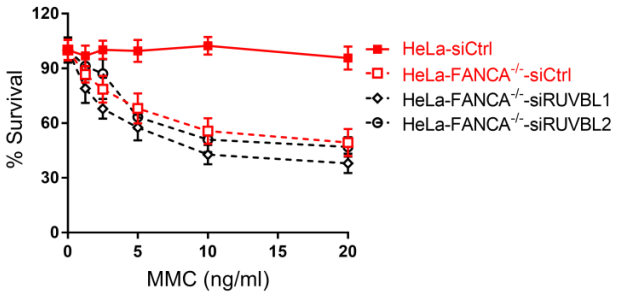

Figure S6

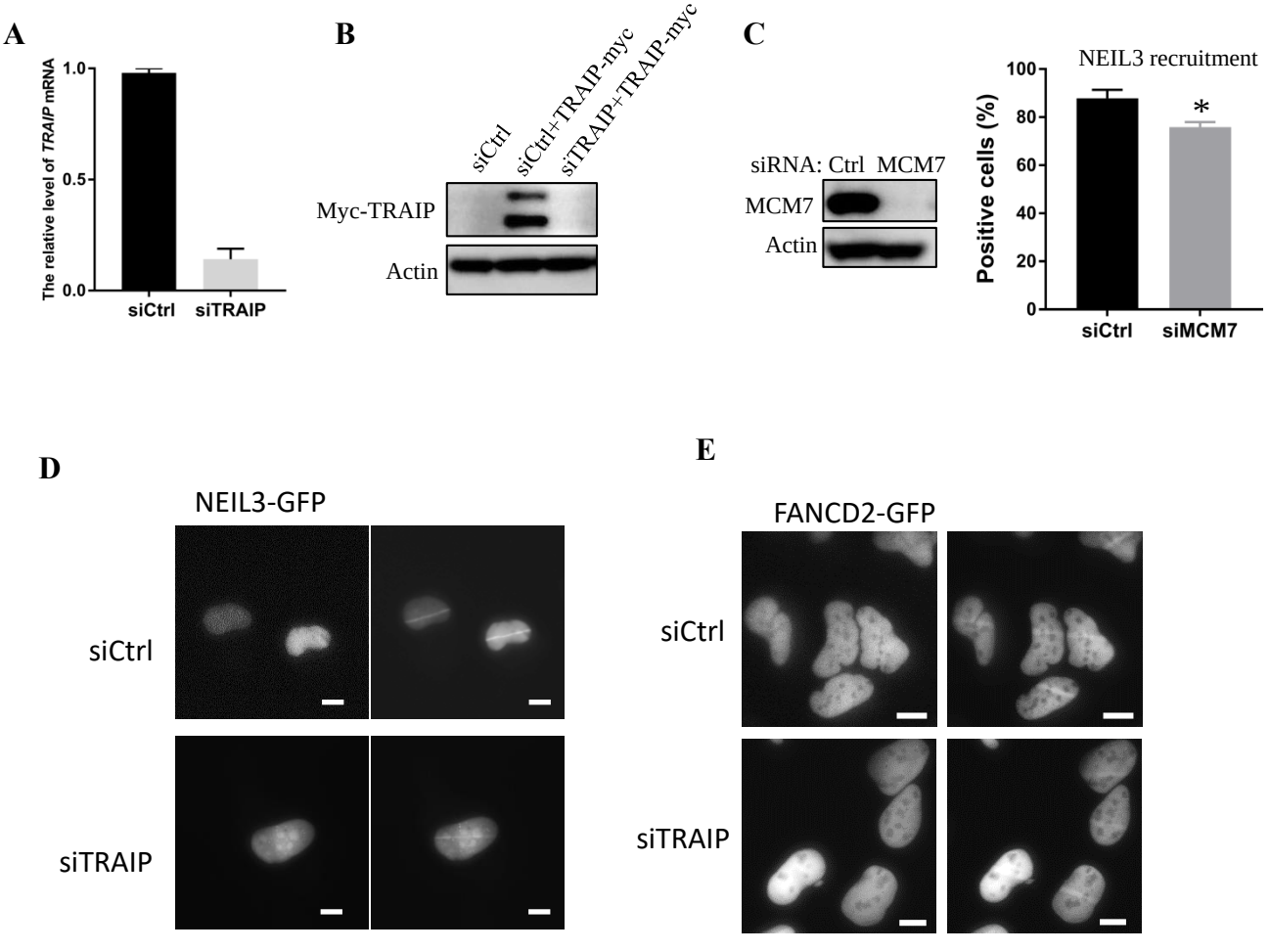
A
The relative level of TRAIP mRNA
1.0
0.5
0.0
siCtrl
siTRAIP
B
siCtrl
siCtrl+TRAIP-myc
siTRAIP+TRAIP-myc
Myc-TRAIP
Actin
C
siRNA: Ctrl MCM7
MCM7
Actin
NEIL3 recruitment
Positive cells (%)
100
80
60
40
20
0
*
siCtrl
siMCM7
D
NEIL3-GFP
siCtrl
siTRAIP
E
FANCD2-GFP
siCtrl
siTRAIP

Table S1. Sequences of the siRNAs used in this study.

Target	Supplier	Sequence
Negative control	Life technologies	GGGUAUCGACGAUUACAAA
NEIL3 #1	Life technologies	GGGUGGAUCAUGUUAUGGA
NEIL3 #2	Life technologies	GCUAAUGGAUCAGAACGUA
NEIL1	Life technologies	CGACUGUUCGUUGGUGCUUAA
FANCA	Life technologies	UUUUUCCCUCUUGACCCUU
FANCD2	Life technologies	GGCUCAGGAUUCUAAUGUA
TRAIP	Life technologies	AGCAGAUGAAGUACUUAGA
PARP1	Dharmacon	siGENOME Human PARP1 siRNA-SMART pool (M-006656-01-0005)
PARP3	Dharmacon	siGENOME Human PARP3 siRNA-SMART pool (M-009297-02-0005)
MCM7	Dharmacon	SMARTpool: ON-TARGETplus MCM7 siRNA (L-003278-00-0005)
RUVBL1	Dharmacon	siGENOME Human RUVBL1 siRNA-SMART pool (M-008977-01-0005)
RUVBL2	Dharmacon	siGENOME Human RUVBL2 siRNA-SMART pool (M-012299-00-0005)